ders. In this study, we conclude that flexural compressive strength does not change for specimens having a length greater than 30.0 cm for C-shaped reinforced concrete specimens as shown in Figure 3.

The modified size effect equation proposed by Kim et al. (1989, 1990) was used as the basic equation for the regression analysis of the experimental results of both length and depth size effect. The predicted depth size effect equation was given as

$$\sigma_N(c) = \frac{Bf_c'}{\sqrt{1+\frac{c}{l_0}\lambda(c)}} + \alpha f_c' \quad (2)$$

where the function $\lambda(c)$ represent the size of fracture process zone with a strain gradient, $l_o$ is the width of crack band which is empirically known to be related to the maximum aggregate size (e.g., $l_o=\lambda_o d_a$ in which $\lambda_o$ is an approximate constant between values of 2.0 and 3.0 (Bazant 1984, Kim et al. 1998, 1999, 2000), $B$ and $\alpha$ are empirical constants of MSEL calculated as 0.70 and 0.47 (Kim et al. 2000), respectively. In the regression analyses, $\lambda_o$ was chosen as 2.0 where $l_o$=2.0×$d_a$=2.0× $d_a$ =2.6 cm.

Due to the microcrack concentration at the failure zone which intensifies the strain gradient, the size effect becomes distinct. More specifically, if the value of $c$ increases, then the strain gradient and size effect decrease. Therefore, it is assumed that the size of $c$ is inversely proportional to the value of $\lambda(c)$. For the case of length dependent size effect, MSEL equation is similar to Equation 2 except that the depth variable $c$ will be replaced by the length variable $h$ where $\lambda(c)$ is then substituted with $\lambda'(h)$.

In order to obtain an analytical equation which predicts the flexural compressive strength of C-shaped specimens for length effect at failure, MSEL is used. Then, Least Square Method (LSM) regression analyses are performed on for the results of the 11 test data for length effect. Equation 3 is obtained from the analyses and the results are graphed and shown in Figure 3.

$$\sigma_N(h) = \frac{0.70 f_c'}{\sqrt{1+\frac{h}{2.6}\left(1.59\left(\frac{1}{h}\right)^{0.37}\right)}} + 0.47 f_c' \; (h/c \le 3.0) \quad (3.a)$$

$$\sigma_N(h) = 0.75 f_c' \qquad (h/c \ge 3.0) \quad (3.b)$$

where nominal flexural compressive strength $\sigma_N$ and uniaxial compressive strength $f_c'$ are in MPa and length of C-shaped specimen $h$ is in cm. If the ratio of length and depth $h/c$ is greater than or equal to 3.0, then this ratio $h/c$ shall be 3.0.

To develop an equation for depth effect, LSM regression analyses are also performed on the 8 results from the depth effect series. All techniques and notations are same as for length effect. Equation 4 is obtained from the analyses and the results are graphically shown in Figure 4.

$$\sigma_N(c) = \frac{0.70 f_c'}{\sqrt{1+\frac{c}{2.6}\left(4.17\left(\frac{1}{c}\right)^{0.53}\right)}} + 0.47 f_c' \quad (4)$$

where depth of C-shaped specimen $c$ is in cm. Figure 3 shows the value $\sigma_N(h)/f_c'$ as a function of the length to depth ratio ($h/c$). And Figure 4 shows the value $\sigma_N(c)/f_c'$ as a function of the depth $c$. The hollow circular data points and the thick solid line in Figures 3 and 4 represent experimental data and analytical results from Equations 3 and 4, respectively. Figure 3 indicates a strong length dependent size effect. Equation 3 shows a good agreement with the experimental results. For a length-to-depth ratio greater than 3.0, the failure strength approaches a constant value of 0.75. Figure 4 shows a distinct depth dependent size effect when normalized with the compressive strength $f_c'$. Equation 4 shows a reasonable agreement with the experimental results.

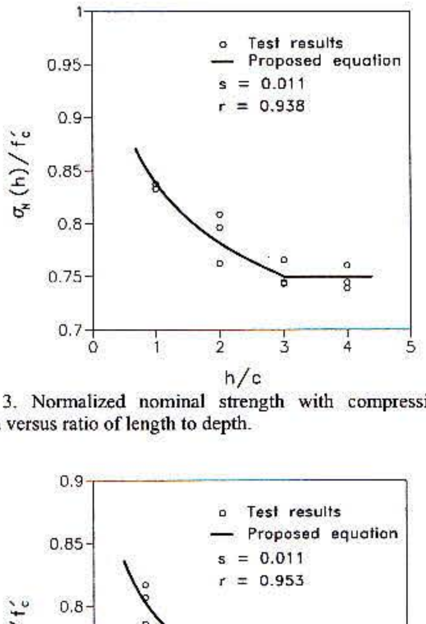


Figure 3. Normalized nominal strength with compressive strength versus ratio of length to depth.

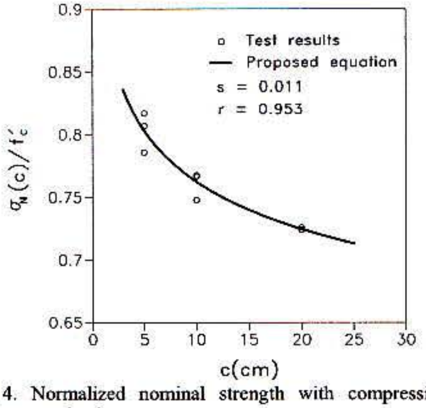


Figure 4. Normalized nominal strength with compressive strength versus depth.

### 3.3 *Generalization of size effect law for C-shaped specimens*

Equation 5 was obtained from LSM regression analysis of 19 new experimental data and 20 previous data (Kim et al. 2000) of which the length to depth ratio $h/c$ value was a constant value of 2.0.

$$\sigma_N(c,h) = \frac{0.70 f_c'}{\sqrt{1+\frac{c}{2.6}\left(0.77\left(\frac{h}{c}\right)^{0.56}-0.13\right)}} + 0.47 f_c' \quad (5)$$

where if $h/c \geq 3.0$, $h/c$ shall be 3.0, and notations are same as in Equations 3 and 4. If the ratio $h/c$ is 2.0, then the value of $\lambda(h/c)$ will be 1.0 and Equation 5 will be same as Equation 1 presented in reference 21 (Kim et al. 2000).

In Figure 5, the thick solid line represents the analytical results obtained using Equation 5 and the hollow circular data points represent the experimental data. The figure shows that Equation 5 agrees with the experimental results quite well. Thus, flexural compressive strength of a beam specimen for various length and depth can be calculated by inputting $c$, $h$, and $f_c'$ into Equation 5.

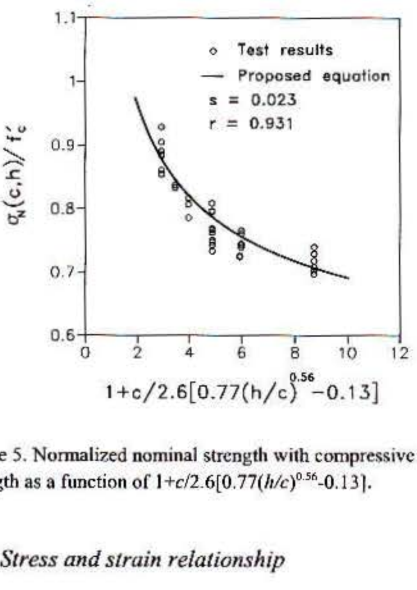


Figure 5. Normalized nominal strength with compressive strength as a function of $1+c/2.6[0.77(h/c)^{0.56}-0.13]$.

### 3.4 *Stress and strain relationship*

Stress values on compressed face $f_c$ obtained from LSM regression analyses using a cubic equation $f_c = A_1 + A_2\varepsilon_c + A_3\varepsilon_c^2 + A_4\varepsilon_c^3$ for length and depth effect of C-shaped specimens are plotted against strain values on compressed face $\varepsilon_c$ in Figures 6a and 6b, respectively. LSM regression analysis was performed on the data points obtained from the experiments based on satisfying force and moment equilibrium around the neutral-axis of cross-section. In other words, in order to perform LSM regression, the values of force, moment, and extreme compression fiber strain $\varepsilon_c$ at every load step are required. LSM regression method minimizes the sum of squares of $m$ nolinear functions $f_i$ of $n$-dimensional vector $x$ (column matrix); $\sum f_i^2(x)$ = Minimum. And the coefficients $A_1$, $A_2$, $A_3$, and $A_4$ are determined. It is assumed that the established $f_c$ and $\varepsilon_c$ relationship is valid for all layers in the section. Thus, a compressive stress can be determined from this relationship using the measured strain values.

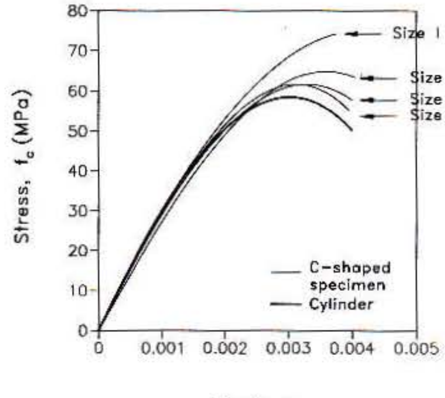


(a) Length effect.

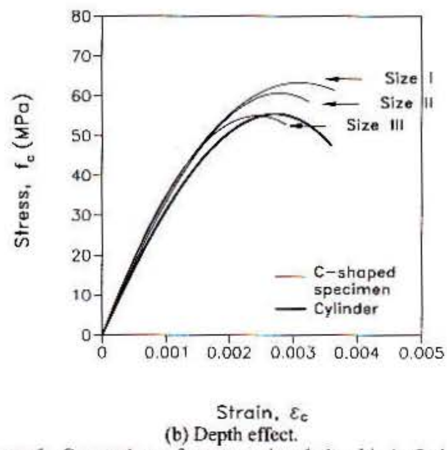


(b) Depth effect.

Figure 6. Comparison of stress-strain relationship in C-shaped specimens and cylinders from experiment.

Also, the thick solid lines in these figures are the uniaxial compressive stress-strain curves obtained from standard concrete cylinder tests. Maximum stress value and the corresponding strain value of C-shaped specimen show a significant increase as the specimen length or depth decreases. For length effect, the maximum stress value and the corresponding strain value of specimen size I is largest when compared to the other specimen sizes.

However, maximum stresses and corresponding strains of C-shaped specimens are relatively similar for specimen sizes III and IV in Figure 6a. The reason for this trend is that flexural compressive strength does not change for specimens having a ratio of length to depth greater than 3.0. For depth size effect, the maximum stress value and the corresponding strain value of specimen size I is largest when compared to the other specimen sizes.

These figures show that there is a brittle failure when concrete with higher strength is used. In order to capture the descending branch of the stress-strain curve, the experiment should be performed using concrete with lower strength. Also, the figures show that stress and strain relationship for concrete in flexural compression may be different from that of a uniaxial compressive strength of cylinders, especially in the descending branch.

### 3.5 *Ultimate strain*

It is generally acknowledged that the ultimate strain of concrete ranges between 0.003 and 0.004 based on many experimental results from beams with rectangular cross section subjected to flexural compressive load. Similar results were also obtained in this study for both length and depth size effect cases. In Figure 7, the thick dashed line represents the ultimate strain of 0.003 suggested by ACI Code and the hollow circular data points represent the test results. It was observed that the ultimate strain of every specimen is greater than 0.003 which is similar to the research results reported by Hognestad et al. (1955), Kaar et al. (1977), Nedderman et al. (1973), Corley (1966). Although there is a minute scattering of data points for larger specimens, the difference is insignificant.

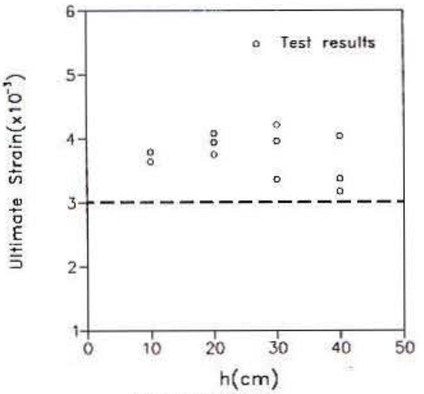


(a) Length Effect.

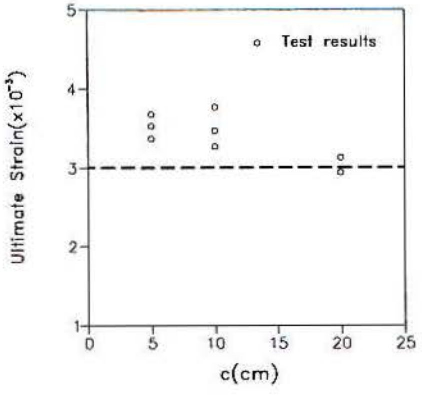


(b) Depth effect.

Figure 7. Comparison of ultimate strain with specimen size.

## 4 CONCLUSIONS

A series of compression tests for 19 C-shaped concrete specimens and cylinders cast from the same batch were performed to evaluate the length and depth effects on the flexural compressive strength of flexural members. From the test results and analyses, the following conclusions are drawn.

1. Length effect is apparent (i.e., the flexural compressive strength at failure decreases as the specimen length increases). Depth effect is also distinct. New parameter values of MSEL are suggested which better predicts the "reduction phenomena" of the strength. More general parameter values are also suggested using the previous data (Kim et al. 2000).
2. For stress and strain relationship, the length and depth effect is also apparent. However, for specimens with a length-to-depth ratio greater than 3.0, length effect of flexural compressive strengths is insignificant. However, it would be desirable in the future to test specimens of broader size ranges.
3. Ultimate strains for both cases range between 0.003 and 0.004. They are similar to general test results for beams and are greater than the value of 0.003 suggested by ACI Code.
4. The results suggest that the current strength criteria based design practice should be reviewed.

## REFERENCES


1. Bazant, Z.P. 1987. Fracture Energy of Heterogeneous Materials and Similitude. *SEM-RILEM International Conference on Fracture of Concrete and Rock*: 390-402.
2. Bazant, Z.P. 1989. Identification of Strain-Softening Constitutive Relation from Uniaxial Tests by Series Coupling Model for Localization. *Cement and Concrete Research* 19: 973-977.

3. Bazant, Z.P. 1984. Size Effect in Blunt Fracture; Concrete, Rock, Metal. *J. of Engineering Mechanics-ASCE* 110(4): 518-535.
4. Bazant, Z.P. 1993. Size Effect in Tensile and Compressive Quasibrittle Failures. *Proc. of the JCI Int. Workshop, Size Effect in Concrete Structures, held in Sendai, Japan, (edited by Mihashi H., Okamura, H. and Bazant, Z.P.), E&FN Spon London*: 161-180.
5. Bazant, Z.P. & Chen, E.P. 1997. Scaling of Structural Failure. *Appl. Mech. Reviews-ASME* 50(10): 593-627.
6. Bazant, Z.P. & Xi, Y. 1991. Statistical Size Effect in Quasibrittle Structures: II. Nonlocal Theory. *J. of Engineering Mechanics-ASCE* 117(11): 2623-2640.
7. Bazant, Z.P., Xi, Y. & Reid, S.G. 1991. Statistical Size Effect in Quasi-brittle Structures: I. Is Weibull theory applicable? *J. of Engineering Mechanics-ASCE* 117(11): 2609-2622.
8. Bazant, Z.P. & Xiang, Y. 1994. Compression Failure of Quasibrittle Materials and Size Effect. *AMD Symp. Ser. ASME Appl. Mech. Div., 185, Damage Mechanics in Composites, ASME Winter Annual Meeting.* Chicago, Allen, D.H. & Ju, J.W., eds,: 143-148.
9. Bazant, Z.P. & Xiang, Y. 1997. Size Effect in Compression Fracture: Splitting Crack Band Propagation. *J. of Engineering Mechanics-ASCE* 123(2): 162-172.
10. Corley, G.W. 1966. Rotational Capacity of Reinforced Concrete Beams. *ASCE Proceedings* 92(5): 121-146.
11. Cotterell, B. 1972. Brittle Fracture in Compression. *Int. J. Fracture Mech.* 8(2): 195-208
12. Gonnerman, H.F. 1925. Effect of Size and Shape of Test Specimen on Compressive Strength of Concrete. *Proc. ASTM* 25: 237-250.
13. Hillerborg, A. 1988. Fracture Mechanics Concepts Applied to Moment Capacity and Rotational Capacity of Reinforced Beams. *Proc. Int. Conf. Fracture and Damage Mechanics of Concrete and Rock, Vienna*: 233-240.
14. Hognestad, E., Hanson, N.W. & McHenry, D. 1955. Concrete Stress Distribution in Ultimate Strength Design. *ACI J.* 52(4): 455-479, also PCA Development Bulletin D6.
15. Jansen, D.C. & Shah, S.P. 1997. Effect of Length on Compressive Strain Softening of Concrete. *J. of Engineering Mechanics-ASCE* 123(1): 25-35.
16. Jenq, Y.S. & Shah, S.P. 1991. Features of Mechanics of Quasi-Brittle Crack Propagation in Concrete. *International Journal of Fracture* 51: 103-120.
17. Kaar, P.H., Hanson, N.W. & Capell H.T. 1977. Stress-Strain Characteristics of High-Strength Concrete. *PCA Research and Development Bulletin RD051.01D*: 1-10.
18. Kim, J.K. & Eo, S.H. 1990. Size Effect in Concrete Specimens with Dissimilar Initial Cracks. *Magazine of Concrete Research* 42(153) 233-238.
19. Kim, J.K., Eo, S.H. & Park, H.K. 1989. Size Effect in Concrete Structures without Initial Crack. *Fracture Mechanics: Application to Concrete, SP-118, ACI* Detroit: 179-196.
20. Kim, J.K., Yi, S.T. & Eo, S.H. 1998. Size Effect of Concrete Compressive Strength for the Non-standard Cylindrical Specimens. *FRAMCOS-3, AEDIFICATIO Publishers*: 1973-1982.
21. Kim, J.K., Yi, S.T. & Kim, J.H.J. 2000. Effect of Specimen Sizes on Flexural Compressive Strength of Concrete. *ACI Structural J.*: (accepted).
22. Kim, J.K., Yi, S.T., Park, C.K. & Eo, S.H. 1999. Size Effect on Compressive Strength of Plain and Spirally Reinforced Concrete Cylinders. *ACI Structural J.* 96(1): 88-94.
23. Kim, J.K., Yi, S.T. & Yang, E.I. 2000. Size Effect on Flexural Compressive Strength of Concrete Specimens. *ACI Structural J.* 97(2): 291-296.
24. Markeset, G. 1995. A Compressive Softening Model for Concrete. Fracture Mechanics of Concrete Structures, (edited by Wittmann F.H.), *FRAMCOS-2* AEDIFICATIO Publishers: 435-443.
25. Markeset, G. & Hillerborg, A. 1995. Softening of Concrete in Compression Localization and Size Effects. *Cement and Concrete Research* 25(4): 702-708.
26. Nedderman, H. 1973. Flexural Stress Distribution in Very High Strength Concrete. *Masters Degree Thesis, Department of Civil Engineering, University of Texas at Arlington.*
27. Rokugo, K. & Koyanagi, W. 1992. Role of Compressive Fracture Energy of Concrete on the Failure Behaviour of Reinforced Concrete Beams. *in Applications of Fracture Mechanics to Reinforced Concrete (ed. A. Carpenteri), Elsevier Applied Science*: 437-464.
28. Swartz, S.E., Nikaeen, A., Narayan Babu, H.D., Periyakaruppan, N. & Refai, T.M.E. 1985. Structural Bending Properties of Higher Strength Concrete. *High-Strength Concrete, SP-87, ACI*: 147-178.
29. Van Mier, J.G.M. 1992. Scaling in Tensile and Compressive Fracture of Concrete. *in Applications of Fracture Mechanics to Reinforced Concrete (ed. A. Carpenteri), Elsevier Applied Science*: 95-135.
30. Vonk, R.A. 1992. Softening of Concrete Loaded in Compression. *Ph. D. thesis Eindhoven University of Technology, the Netherlands.*